

Title	Shape-related useful properties of nanostructured thin films
Author(s)	Suzuki, Motofumi
Citation	AIP Conference Proceedings: NATIONAL PHYSICS CONFERENCE 2014 (PERFIK 2014) (2015), 1657: 030003
Issue Date	2015-04-25
URL	http://hdl.handle.net/2433/210551
Right	© 2015 AIP Publishing LLC
Type	Conference Paper
Textversion	publisher

Shape-related useful properties of nanostructured thin films

Motofumi Suzuki

Citation: [AIP Conference Proceedings](#) **1657**, 030003 (2015); doi: 10.1063/1.4915153

View online: <http://dx.doi.org/10.1063/1.4915153>

View Table of Contents: <http://scitation.aip.org/content/aip/proceeding/aipcp/1657?ver=pdfcov>

Published by the [AIP Publishing](#)

Articles you may be interested in

[Comparative study of the mechanical properties of nanostructured thin films on stretchable substrates](#)

J. Appl. Phys. **116**, 093504 (2014); 10.1063/1.4894616

[Optoelectronic Properties of Nanostructured Cadmium Sulphide Thin Films](#)

AIP Conf. Proc. **1391**, 585 (2011); 10.1063/1.3643618

[Optical, structural, and magnetic properties of cobalt nanostructure thin films](#)

J. Appl. Phys. **105**, 113508 (2009); 10.1063/1.3138809

[Optical and electrical properties of nanostructured LaCoO₃ thin films](#)

Appl. Phys. Lett. **87**, 061909 (2005); 10.1063/1.2009057

[Structure-related optical properties of thin films](#)

J. Vac. Sci. Technol. A **4**, 418 (1986); 10.1116/1.573894

Shape-Related Useful Properties of Nanostructured Thin Films

Motofumi Suzuki

Department of Micro Engineering, Kyoto University, Kyoto 615-8540, Japan

Abstract. The recent status of practical applications of obliquely deposited thin films is reviewed. Owing to the anisotropy in polarizability of elongated nanocolumns, obliquely deposited thin films in the form of assemblies of aligned nanocolumns show anisotropies in various properties, such as birefringence, dichroism, and magnetism. In addition, we introduce examples of practical applications: thin film waveplates, angular selective coatings, Au nanorod arrays for surface-enhanced Raman scattering, and low-reflectivity wire-grid polarizers.

Keywords: glancing angle deposition; practical applications; shadowing growth.

PACS: 68.55.-a, 68.70.+w, 78.20.Fm, 78.67.Bf, 78.67.Rb

INTRODUCTION

According to elementary electromagnetic theory, dielectric and magnetic polarization phenomena are strongly influenced by the shape of a body, i.e., easy polarization along the elongated side [1, 2]. The collective response of well-aligned elongated elements shows various anisotropies in optical [3-5], electrical [6], magnetic [7, 8], and mechanical properties [9] resulting from the shape of the constituent elements. For example, a photonic metamaterial with elongated elements that are much smaller than the optical wavelength exhibits optical anisotropies such as birefringence [3, 4] and dichroism [10, 11], regardless of the crystallinity of each element. One of the most powerful methods to prepare such metamaterials having shape-related useful properties is the so-called dynamic oblique deposition (DOD) technique [12, 13], in which a substrate is set obliquely or sometimes rotated in-plane. Through DOD, unique nanocolumnar structures have been prepared by means of the self-shadowing effect and the limited mobility of adatoms. Considerable progress has recently been made in developing products by the DOD technique.

In this presentation, we will discuss the fundamentals of shape-related properties and the DOD technique. We will also introduce our recently commercialized products developed by DOD, namely surface-enhanced Raman substrates [14, 15], thin-film waveplates [16], and low reflectivity wire-grid polarizers [11]. Because DOD films exhibit great potential to overcome the energy and environmental problems confronting humankind, the use of these films in industries should be encouraged by eliminating any negative prejudice against these films.

ORIGIN OF ANISOTROPY

Figure 1 shows typical examples of DOD thin films [17]. During conventional PVD, the vapor is deposited on a substrate from the normal direction in vacuum so that flat, uniform thin films are produced. In contrast, during DOD, the substrate is set obliquely and sometimes rotated in-plane, as shown in Fig. 1(g). If the substrate temperature is sufficiently low, unique nanocolumnar structures such as zigzags, helices, posts, and complex hybrid structures are created [Fig. 1(a)–1(e)]. The physical origins of the columnar structure in DOD thin films are self-shadowing effects and the limited mobility of the deposited atoms. When the vapor flux is obliquely incident on the substrate surface, atoms in the growing films shadow unoccupied sites from the direct sticking of incident atoms (“shadowing effect”). Moreover, owing to limited mobility, the unoccupied sites are not filled later. As a result, oblique columns grow in the direction of the incident vapor beam.

The columnar structures can be modeled as an assembly of elongated nanoellipsoids as shown in Fig. 2(a) [5]. Let us consider polarization properties of each nanoellipsoid (Fig. 2(b)) as expressed by the following equation,

$$\frac{x^2}{a_1^2} + \frac{y^2}{a_2^2} + \frac{z^2}{a_3^2} = 1. \quad (1)$$

When an ellipsoid with dielectric constant ε_p is embedded in a medium with dielectric constant ε_m and a uniform electric field is applied, the polarizability α_i ($i=1, 2, 3$) is written as [1, 2]

$$\alpha_i = 4\pi a_1 a_2 a_3 \frac{\varepsilon_p - \varepsilon_m}{3\varepsilon_m + 3L_i(\varepsilon_p - \varepsilon_m)}, \quad (2)$$

where L_i is the geometric factor and is written as

$$L_i = \frac{a_1 a_2 a_3}{2} \int_0^\infty \frac{dq}{(a_i^2 + q)f(q)}, \quad (3)$$

$$f(q) = \sqrt{(q + a_1^2)(q + a_2^2)(q + a_3^2)}. \quad (4)$$

In the case of a needle-like nanospheroid ($\alpha_1 \gg \alpha_2 = \alpha_3$), $L_1 = 0$ and $L_2 = L_3 = 1/2$, so the nanospheroid is easy to polarize along the elongated direction. Therefore, in the form of an assembly of unidirectionally aligned nanospheroids, nanocolumnar thin films show biaxial anisotropy in their optical, electrical, and magnetic properties.

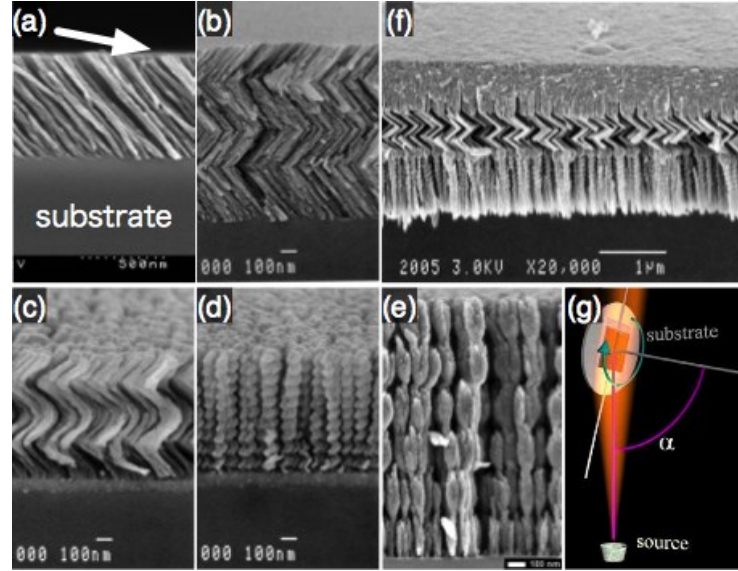


FIGURE 1. (a)–(f) Typical examples of the nanocolumnar structures of oblique-angle deposited (OAD) thin films, (g) a schematic drawing of the deposition geometry [17].

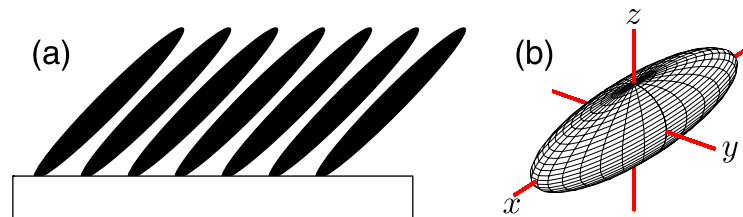


FIGURE 2. (a) Oblique columnar structure as an assembly of elongated spheroids, (b) dielectric spheroid.

PRACTICAL APPLICATIONS OF SHAPE-RELATED USEFUL PROPERTIES

Thin Film Waveplates [16, 18]

Oblique columnar thin films of a transparent material show large birefringence ($\Delta n \sim 0.5$ or larger) at a deposition angle of around 70° [4]. This property is quite useful for application in thin film waveplates. Fig. 3 shows photographs of a Ta_2O_5 waveplate deposited in 1998 [18] and kept in ambient conditions in the author's office for more than 10 years. This film was deposited by using the Motohiro-Taga process [4] at a deposition angle of 70° and has a chevron-shaped columnar cross section. As indicated in Fig. 3(a), the film is completely transparent. From the photograph taken through polarizers shown in Fig. 3(b), it is clear that the retardation properties are quite uniform. Therefore, the film is very durable and exhibits high uniformity over an area of 100 cm^2 . In addition, such a film is well reproducible because it was prepared by physical processes. Hodgkinson and Wu [19] succeeded in enhancing the birefringence by using a so-called serial bideposition technique, and very recently, Koike et al. [16] have developed practical thin film waveplates for optical pickups and liquid crystalline projectors.

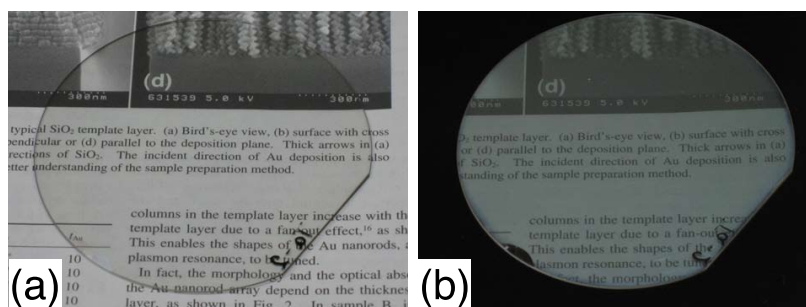


FIGURE 3. Visual appearance of a waveplate of an oblique-angle deposited (OAD) Ta_2O_5 thin film [18] taken (a) without and (b) with commercial sheet polarizers.

Angular Selective Coatings [10]

For the obliquely codeposited thin films with small metal particles are expected for the angular-selective coatings [10]. Oblique columnar thin films containing small metal particles show anisotropy in optical absorption depending on the polarization of the incident light and the angle of incidence. Small Ag particles can be embedded in the oblique columnar SiO_2 by oblique codeposition [10]. The anisotropic transmittance properties for the obliquely codeposited Ag- SiO_2 are shown in Fig. 4(a). Measurements of the transmittance were performed in the plane of the vapor incidence as shown in Fig. 4(b). All spectra have absorption bands at wavelengths between 330 and 600 nm. This large optical anisotropy in the obliquely codeposited Ag- SiO_2 thin films was explained in terms of the plasma resonance of Ag particles embedded in an anisotropic medium. Figures 4(c) and (d) are the visual appearances of Ag- SiO_2 thin films viewed from $\theta = +45^\circ$ and $\theta = -45^\circ$. They show clear, significant angular selectivity and may be useful for the coatings of inclined windows.

Noble Metal Nanorod Arrays for SERS [14, 15]

Much attention has been devoted to surface-enhanced Raman scattering (SERS) in the near-IR (NIR) region from the viewpoint of biochemical sensor applications. For application to biological materials, excitation in the NIR region is appropriate because this region is compatible with biological tissues' transparency window. Elongated nanoparticles (so-called nanorods) are strong candidates for NIR SERS substrates because the local field can be significantly enhanced at their ends. We have succeeded in aligning the nanorods end to end by using DOD [20]. Figure 5(a) shows the morphology of our Au nanorod arrays. Au nanorods were aligned on a SiO_2 template layer (called the "shape control layer") having an anisotropic surface morphology prepared by oblique angle deposition (OAD) [15]. The shape control layer of SiO_2 as the template for Au nanorods is prepared by a serial bideposition (SBD) technique. The surface of the shape control layer prepared by SBD is corrugated anisotropically. On the anisotropic shape control layer, Au is also evaporated obliquely in vacuum. The deposited Au is only around 10 nm thick on average. The Au sticks only to the top of the columns, owing to shadowing, and forms elongated

nanoparticles (nanorods). Due to the in-line alignment of nanorods, the nanorod arrays show large dichroism in the NIR region corresponding to the local plasmon resonance, as shown in Fig. 5(b). Excellent SERS properties are observed, as indicated in Fig. 5(c), when Raman spectra are measured on Au nanorod arrays immersed in a solution of 4,4'-bipyridine. The SERS spectra can be detected down to $1\text{ }\mu\text{M}$ of solution within a few minutes after the immersion of samples. In our measurement system, the spot size of the laser is around $1\text{ }\mu\text{m}^2$. The thickness of the nanorod array is of the order of 10 nm . Therefore, at $1\text{ }\mu\text{M}$, the number of molecules existing inside the SERS active volume is estimated to be fewer than 10 molecules. Thus, our nanorod arrays are nearly sensitive enough to detect a single molecule. The high sensitivity can be attributed to the high number density of nanorods and effective field concentration between in-line aligned nanorods.

In addition to the high sensitivity, our nanorod arrays are well reproducible, and no contamination occurs during deposition. Moreover, they maintained high SERS sensitivity for more than one year. These are the advantages of the OAD technique. Fortunately, a Japanese coating company recently began to produce our nanorod arrays. These are already available on the market today.

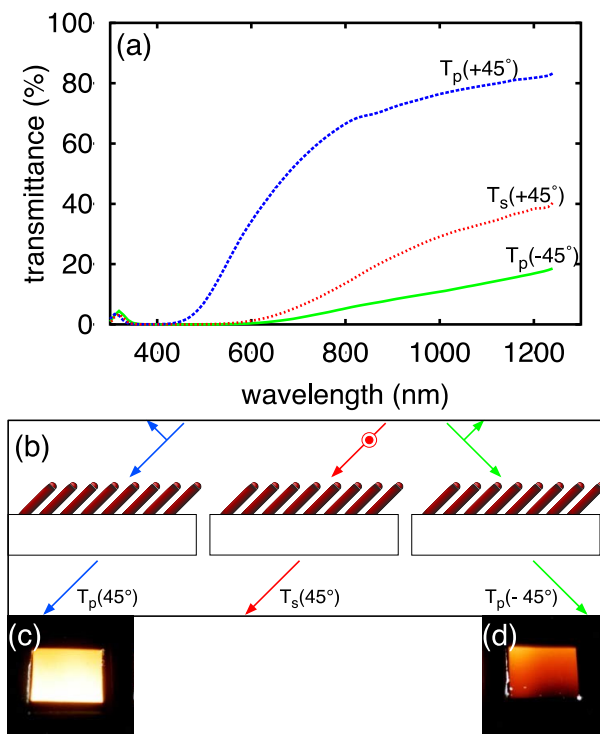


FIGURE 4. (a) Transmittance spectra of the Ag-SiO₂ angular selective coating, (b) definition of measurement geometry, (c) and (d) visual appearances at $+45^\circ$ and -45° , respectively [10].

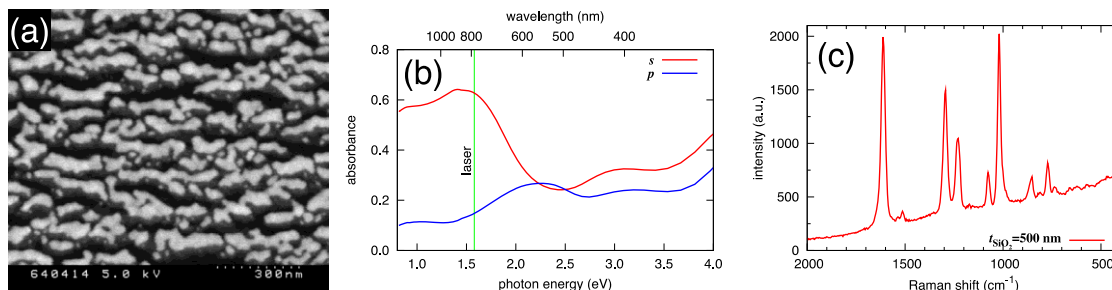


FIGURE 5. (a) Scanning electron microscopy image of the surface, (b) polarization-dependent absorbance spectra, and (c) surface-enhanced Raman scattering spectra of the Au nanorod array [15].

Low-Reflectivity Wire-Grid Polarizers [11]

Recent liquid-crystal (LC) projectors require high thermal durability for their optical elements. Metal wire-grid (WG) polarizers are quite suitable because they are not degraded by heat and light. In addition, high reflectivity of the wire-grid polarizers is useful for recycling the light near the light source. However, highly reflective polarizers downstream might generate stray light, which might degrade image quality. Thus, improving the brightness and durability of projectors requires the development of low-reflectivity (LR) WG polarizers.

From considerations based on optical admittance, we found that the reflectivity of conventional WG polarizers can be reduced if we fabricate the multilayered wires of absorptive and dielectric materials on highly reflective Al wires. At first, we prepare aluminum WG polarizers by interference lithography and dry etching. The dielectric layer of SiO_2 is deposited by ordinary sputtering. The absorptive layer of FeSi_2 is then deposited by ion beam sputtering at a glancing deposition angle of 87° from the surface normal. Because of the shadowing effect, the sputtered FeSi_2 adheres only to the top of the WGs covered with SiO_2 .

Figures 6(a) and (b) indicate the reflectance and transmittance spectra of a WG and an LR-WG polarizer. The reflectance of TE waves for the LR-WG polarizer is clearly much smaller than that for the WG polarizer. No significant degradation of the transmission properties is recognized. In Figs. 6(c) and (d), the visual appearances of these polarizers are displayed. These photos are taken through a commercial sheet polarizer of which the polarization axis is perpendicular (Fig. 6(c)) or parallel (Fig. 6(d)) to wires. The LR-WG polarizer clearly looks much darker than the WG polarizer. The durability of the LR-WG polarizers is basically identical to that of the conventional WG polarizers. Our LR-WG polarizers are now used in commercial LC projection displays that require high thermal durability.

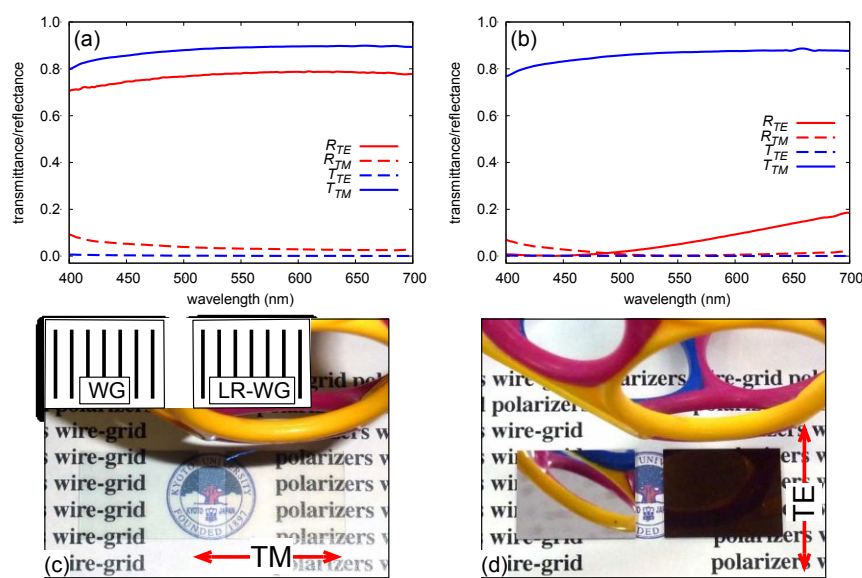


FIGURE 6. (a) and (b) Transmittance/reflectance spectra of wire-grid (WG) and low-reflectivity WG (LR-WG) polarizers, respectively. (c) and (d) Visual appearances of WG/LR-WG polarizers taken through a commercial sheet polarizer, the polarization axis of which is perpendicular (c) and parallel (d) to the wire grids [11].

SUMMARY

Unique nanocolumnar morphologies can be tailored by the DOD technique. Many of the shape-related useful properties of DOD thin films originate from the anisotropy in polarizability of elongated nanocolumns. In this article, examples of such shape-related properties have been reviewed. Applications include thin film waveplates, angular selective coatings, and noble metal nanorod arrays for SERS and LR-WG polarizers. Because tailoring nanomorphology by DOD is robust in selection of materials, more advanced applications are expected by integrating the functions of nanoshapes as well as functions of materials.

ACKNOWLEDGMENTS

This article has been prepared in collaboration with all members of the Micro Process Engineering Laboratory at Kyoto University, Akio Takada and Nobuyuki Koike at Dexerials Corporation, and Yasunori Yaga at Chubu University, Japan. Student contributions were especially important for carrying out the investigations. I am also grateful to Sadamu Kinoshita of Kyoto University for the SEM observations. This work was supported by KAKENHI 25286037, 21656058, and 17310073.

REFERENCES

1. H.C. van de Hulst, *Light Scattering by Small Particles*, New York: Dover, 1981.
2. C.F. Bohren, D.R. Huffman, *Absorption and Scattering of Light by Small Particles*, New York: Wiley, 1983.
3. H.A. Macleod, *J. Vac. Sci. Technol. A* **4**, 418 (1986).
4. T. Motohiro, Y. Taga, *Appl. Opt.* **28**, 2466 (1989).
5. G.B. Smith, *Opt. Commun.* **71**, 279 (1989).
6. K. Kuwahara, H. Hirota, *Jpn. J. Appl. Phys.* **13**, 1093 (1974).
7. E.W. Pugh, J. Matisoo, D.E. Speliotis, E.L. Boyd, *Journal of Applied Physics* **31**, S293 (1960).
8. R. Sugita, *IEEE. Trans. Magn.* **MAG-20**, 687 (1984).
9. R. Gontarz, Ratajczak, H. P. Suda, *Physica Status Solidi* **15**, 137 (1966).
10. M. Suzuki, Y. Taga, *J. Appl. Phys.* **71**, 2848 (1992).
11. M. Suzuki, A. Takada, T. Yamada, T. Hayasaka, K. Sasaki, E. Takahashi, S. Kumagai, *Nanotechnology* **21**, 175604 (2010).
12. K. Robbie, M.J. Brett, A. Lakhtakia, *J. Vac. Sci. Technol. A* **13**, 2991 (1995).
13. M. Suzuki, Y. Taga, *Jpn. J. Appl. Phys. Part 2* **40**, L358 (2001).
14. M. Suzuki, W. Maekita, Y. Wada, K. Nakajima, K. Kimura, T. Fukuoka, Y. Mori, *Appl. Phys. Lett.* **88**, 203121 (2006).
15. M. Suzuki, K. Nakajima, K. Kimura, T. Fukuoka, Y. Mori, *Analytical Sciences* **23**, 829 (2007).
16. N. Koike, K. Sasaki, T. Yamada, N. Hanashima, A. Takada, M. Suzuki, *Journal of Nanophotonics* **8**, 083991 (2014).
17. M. Suzuki, *Journal of Nanophotonics* **7**, 073598 (2013).
18. M. Suzuki, T. Ito, Y. Taga, *Proc. SPIE* **3790** (1999) 94.
19. I. Hodgkinson, Q.H. Wu, *Appl. Opt.* **38**, 3621 (1999).
20. M. Suzuki, W. Maekita, K. Kishimoto, S. Teramura, K. Nakajima, K. Kimura, Y. Taga, *Jpn. J. Appl. Phys. Part 2* **44**, 1193 (2005).